Mon. Not. R. Astron. Soc. **000**, 000–000 (0000) Printed 8 October 2009 (MN LATEX style file v2.2)

Hurst parameter analysis of radio pulsar timing noise

X. S. Na[1], N. Wang[2], J. P. Yuan[2], Z. Y. Liu[2], J. Pan[3] and R. X. Xu[1]
[1] *School of Physics and State Key Laboratory of Nuclear Physics and Technology, Peking University, Beijing 100871, China*
[2] *Urumqi Observatory, National Astronomical Observatories, 40-5 South Beijing Road, Urumqi, 830011, China*
[3] *Purple Mountain Observatory, 2 West Beijing Road, Nanjing 210008, China*

8 October 2009

ABSTRACT
We present an analysis of timing residual (noise) of 54 pulsars obtained from 25-m radio telescope at Urumqi Observatory with a time span of $5 \sim 8$ years, dealing with statistics of the Hurst parameter. The majority of these pulsars were selected to have timing noise that look like white noise rather than smooth curves. The results are compared with artificial series of different constant pairwise covariances. Despite the noise like appearance, many timing residual series showed Hurst parameters significantly deviated from that of independent series. We concluded that Hurst parameter may be capable of detecting dependence in timing residual and of distinguishing chaotic behavior from random processes.

Key words: pulsars: general – methods: statistical

1 INTRODUCTION

All pulsars show a remarkable uniformity of rotation rate on a time scale of a few days as expected of an isolated spinning body with large stable moment of inertia. (Lyne & Smith 2006) The angular momentum of radio pulsar is slowly decreasing through slowdown torque of the magnetic dipole radiation. However, some very interesting irregularities in pulsar rotation have been observed which are termed as *timing noise*.

It is anticipated that valuable information of many interesting physical processes related to pulsars is coded in the timing noises, thus employing statistical measures to characterize timing noises is important to the study of pulsars and thus the properties of the matter at supra-nuclear densities. Efforts to quantify timing noise have been tried as early as timing noise was firstly recognized, for instance according to random walk of different quantities (Boynton et al. 1972), most current models such as vortex creeping are still restricted to treatment of timing noise only as random process in certain quantities. One exception was presented by (Harding et al. 1990), who analyzed timing data of Vela pulsar to look for evidence of chaotic behavior by "correlation sum" technique to estimate fractal dimension of the system. However, despite possible suggestions they concluded that "correlation sum" estimator may be unable to distinguish between random and chaotic processes.

However, any statistical representation of data has their own biases, employing a large types of statistical measures is essentially vital to a fair understanding of the timing noises. Furthermore, the number of observed pulsars has accumulated to $\sim 10^3$ (Manchester et al. 2006) but collected data is often incomplete for a conclusive analysis, it is therefore crucial to diagnose current available but limited data, the results of which could guide us in future observation to concentrate on those pulsars with anomalous timing noise. Here we are introducing a statistical method rarely used in time domain astronomy – the Hurst parameter analysis, which is actually sensitive to the type of the inherent correlation among the time series. Our practical analysis of the timing data observed by the 25-meter radio telescope at Urumqi Observatory of 54 pulsars indicates that Hurst parameter analysis might be capable of detecting anomalous signals which disguise themselves as noises.

2 THE HURST PARAMETER ANALYSIS

2.1 Basic concepts

The timing noise in essence is a discrete realization of a continuous random process $\{X_t\}$, let $\{X_1, X_2, \ldots, X_n, \ldots\}$ be a discrete time series sampled sequentially at time points $t_1, t_2, \ldots, t_n, \ldots$ and the task is to analyze the record $\{X_n\}$ and identify corresponding characteristics of $\{X_t\}$.

The first property one may check is whether there is correlation among the series. The most commonplace time series is the *independently distributed random series* if the covariance $\mathrm{Cov}(X_i, X_j) = 0$ for any $i \neq j$. The independently distributed random series is also the well known as *white noise* for its constant power spectrum. A closely related concept is the colored noises which are called so for their power-law shaped power spectrum $P(k) \propto k^n$ $(n \neq 0)$.

Another important aspect is stationarity. Station-

ary means that for any d indices $k_1, \ldots, k_d$ the vectors $(X_{k_1}, \ldots, X_{k_d})$ and $(X_{k_1+n}, \ldots, X_{k_d+n})$ have the same n-point distribution (Dieker 2004). To ensure the stationarity, one can either enlarge the observation window to have sufficiently long record of data to include the short-term variation, or construct a new set of data by de-trending the observed time series with appropriate models.

If for the new series that sums m consecutive variable $Y_k = X_{km} + X_{km+1} + \ldots + X_{km+m-1}$, there exists a scaling function $a(m)$ so that for any d indices $k_1, \ldots, k_d$ the vectors $(X_{k_1}, \ldots, X_{k_d})$ and $a(m)(Y_{k_1}, \ldots, Y_{k_d})$ have the same n-point distribution, we call the time series *self-similar*. (Dieker 2004) Self-similar time series thus looks the same after scaling up to a factor $a(m)$ while m plays the role of resolution. If for self-similar series the function $a(m)$ obeys power law $a(m) \propto m^{-H}$, we call the series a self-similar series with a *Hurst parameter* of H.

It is obvious that an independently and identically distributed[1] Gaussian series is self-similar with Hurst parameter $H = 1/2$. But once the series has some non-trivial correlation structures, the Hurst parameter may differ from $1/2$, which is better illustrated with the following introduction of Hurst parameter (Feder 1988) for continuous-time stochastic process. If $X(t)$ is a random process on some probability space such that:

(i) with probability 1, $X(t)$ is continuous and $X(0) = 0$;
(ii) for any $t \geqslant 0$ and $\tau > 0$, the increment $X(t+\tau) - X(t)$ follows a normal distribution with mean zero and variance τ^{2H}, so that

$$P\left(X(t+\tau) - X(t) \leqslant x\right) = \frac{\tau^{-H}}{\sqrt{2\pi}} \int_{-\infty}^{x} e^{-u^2/2\tau^{2H}} du \ . \quad (1)$$

The parameter H is then the Hurst parameter (or Hurst exponent), if $H = 1/2$, the random process is just the i.i.d Gaussian random process (c.f. Feder 1988). It is easy to see that the correlation

$$\langle X(t)\left[X(t+\tau) - X(t)\right]\rangle = \frac{(t+\tau)^{2\alpha} - t^{2\alpha} - \tau^{2\alpha}}{2} \quad (2)$$

does not vanish unless $H = 1/2$.

Random walk can be formed from a random process X via $\int X(t)dt$ or $\sum_i X_i$, the random walk with pace length drawn from i.i.d Gaussian series is the normal Brownian motion while those walks coming from Eq. 1 with $H \in (0, 1)$ and $H \neq 1/2$ is named *fractional Brownian motion*. As can be seen from Eq.2, a fractional Brownian motion with Hurst parameter $H > 1/2$ contains a positive correlation between consecutive steps or in other words a persistent trend, and covers wider range than normal Brownian motion (Steeb et al. 2005). For series with $H < 1/2$ the generated random walk will cover less than Brownian motion, implying a negative correlation between consecutive variables or in other words a self-reverting trend, i.e. being *anti-persistent*. Therefore, estimation of Hurst parameter can probe correlation inside the series, i.e. how the 'memory' of its past affects the future. The method was named after its proposer H. Hurst (Hurst 1951), and has been widely used in various areas such as biology, medical science, seismology, and economics.

[1] All random variables within the series have the same distribution and are independent with one another, abbreviated as i.i.d.

2.2 Estimation of the Hurst exponent

Our algorithm is a slightly modified version of the popular Range Over Standard deviation (ROS) algorithm (Steeb et al. 2005) to account for the non-uniform sampling[2]. The timing noise record $X_1, X_2, \ldots, X_N$ taken at time $t_1, \ldots, t_N$, is firstly split into n segments of length $\Delta t_n \approx (t_N - t_1)/n$, i.e. $\{X_N\}$ is re-grouped in the way

$$X_1, \ldots, X_{\ell_1}; X_{\ell_1+1}, \ldots, X_{\ell_2}; \quad \ldots \quad ; X_{\ell_{n-1}+1}, \ldots, X_N$$

so that

$$t_{\ell_i}, t_{\ell_i+1}, \ldots, t_{\ell_{i+1}-1} \in [t_1 + (i-1)\Delta t, t_1 + i\Delta t) \quad (3)$$

For i-th segment $\{X_{\ell_i}, \ldots, X_{\ell_{i+1}-1}\}$ for example, we calculate average A_i and standard deviation S_i of the record $\{0, X_{\ell_i+1} - X_{\ell_i}, \ldots, X_{\ell_{i+1}-1} - X_{\ell_i}\}$ to form a new series $\{Y_{\ell_i}, \ldots, Y_{\ell_{i+1}-1}\}$ whose element is given by

$$Y_{\ell_i+k} = \frac{1}{S_i}\left(X_{\ell_i+k} - A_i\right) \ . \quad (4)$$

The *range* $R_i^{(n)}$ is defined to be the difference between the maximum and the minimum of the accumulated series,

$$\begin{aligned} Z_k^{(i)} &= \sum_{j=1}^{k} Y_{\ell_i+j} \quad (k \leqslant \ell_{i+1} - \ell_i - 1) \\ R_i^{(n)} &\equiv \mathrm{Max}(Z_{k=1,\ldots}^{(i)}) - \mathrm{Min}(Z_{k=1,\ldots}^{(i)}) \end{aligned} \quad (5)$$

where superscript n is the number of segments, and for each n there is an averaged range

$$R^{(n)} = \frac{1}{n}\sum_{i=1}^{n} R_i^{(n)} \ . \quad (6)$$

Therefore for $n = 1, 2, \ldots, n_{\max}$ we obtain a sequence $\{(\Delta t_n, R^{(n)})\}$. $n_{\max}$ is chosen so to be the largest segment number to ensure that every segment contain at least 5 data points. To estimate the power-law index we then use linear regression to fit $\{(\log \Delta t_n, \log R^{(n)})\}$ for the slope as estimation of the Hurst parameter H.

2.3 Simple Monte-Carlo simulation

However there two complications in practical estimation of Hurst parameter of timing residual data:

(i) The algorithm is for series of exact values while for timing noise looks like white noise, uncertainties are usually not negligible.
(ii) The algorithm uses running maximum while the definition uses variance. These two should show the same trend in $n \to \infty$ limit (Karatza et al. 1991) but there is no information to what extend this is true for finite sequence.

In order to control possible systematical effects, we carry out numerical test with simple simulations. [3] We generate 10^3 series $\{(t_n, X_n)\}$ for each pulsar to take error bar

[2] We divide the series into segments of roughly equal time span instead of equal number of data points because usually radio pulsar TOA measurements are not uniform.
[3] In all Monte-Carlo simulations in this article we used Mersenne Twister with a period of $2^{19937} - 1$ for pseudo-random number generator (Matsumoto & Nishimura 1998).

effect into account where n labels data points number and in each sequence X_n follows the Gaussian distribution with standard deviation equal to data error bar lengths and expectation equal to the centers of data error bar. Then Hurst parameters H of these series and their average and standard deviation is calculated for each pulsar.

Next we generate artificial (anti-)persistent series $\{(t_n, Y_n^{(c)})\}$ with constant covariance c between consecutive pair at observation times t_n in order to control systematic error from finite length. In other words, we generate a Gaussian random number $Y_1^{(c)} \sim N(0,1)$ at t_1, then with the value of $Y_1^{(c)}$ we generate independent random number $Y_2^{(c)} \sim N(cY_1^{(c)}, 1)$ for t_2, and so forth for the rest of t_n there is the $Y_n^{(c)} \sim N(cY_{n-1}^{(c)}, 1)$ where c is clearly the constant covariance between consecutive numbers. Then we estimate the Hurst parameter $H^{(c)}$ for each of these series $\{Y^{(c)}\}$. These values would serve as a standard for us to compare with H obtained above.

Note that these series is self-similar but do not have power-law scaling function and therefore do not have a strictly defined Hurst parameter. This can be shown by a simple calculation. Given an i.i.d. series with standard Gaussian distribution $(X_1, X_2, \ldots, X_n, \ldots)$, the process with covariance c can be expressed as

$$(Y_1 = X_1, Y_2 = cX_1 + X_2, \ldots, Y_k = \sum_{k=1}^{n} c^{n-k} X_k, \ldots)$$

and variance of sum of first n variables is

$$\mathrm{Var}\left(\sum_{i=1}^{n} Y_i\right) = \sum_{m=0}^{n-1}\left(\sum_{k=0}^{m} c^k\right)^2 = \alpha c^{2n+1} + \beta c^{n+1} + \gamma n + \delta \tag{7}$$

with

$$\begin{cases} \alpha &= -\frac{1}{(1+c)(1-c)^3} \\ \beta &= \frac{2}{(1-c)^3} \\ \gamma &= \frac{1}{(1-c)^2} \\ \delta &= -\frac{c(c+2)}{(1+c)(1-c)^3} \ . \end{cases} \tag{8}$$

Hence its scaling function is

$$a(n)^2 = \frac{1}{\alpha c^{2n+1} + \beta c^{n+1} + \gamma n + \delta} \tag{9}$$

Clearly it is not power-law except for $c = 0$ which leads to $a(n) \propto n^{-1/2}$. However, we can still use linear regression to find slope $-H$ of the log-log curve of $a(n)$ which gives $H = 0.43, 0.47, 0.56, 0.74$ for $c = -0.8, -0.4, 0.4, 0.8$, $n = 1 \sim 100$, and $H = 0.45, 0.48, 0.54, 0.67$ for $c = -0.8, -0.4, 0.4, 0.8$, $n = 1 \sim 200$. Thus these series can simulate (anti-)persistent series with short length. For long length series with $c < 1$, $a(n)$ will quickly approach $n^{-1/2}$ as $n \to \infty$, in other word $H = 1/2$ in the large n limit. This simply calculation also demonstrates that Hurst parameter deviation from 1/2 seen in long series cannot be attributed only to covariance between only consecutive pairs but reveals long-range dependence which is an essential feature of fractional Brownian motion.

3 PRACTICAL DATA ANALYSIS

3.1 The sample of observed timing noises

Data used in this work is 5 $\sim$ 8 years of timing residual data from 25m radio telescope at Urumqi Observatory. Timing data is processed using standard pulsar software packages PSRCHIVE (Hotan et al. 2004) and TEMPO2 (Hobbs et al. 2006) to obtain timing residual. Time of arrival (TOA) of radio pulse is fitted using PSRCHIVE software from observation data by an input accumulated pulse profile. TEMPO2 software use coordinate system conversion parameters that account for various effects (Roemer delay, Einstein delay, Shapiro delay etc.) and pulsar parameters (P, $\dot{P}$ etc.) to establish a model to predict arrival time of pulses. Timing residual is obtained as difference between observation and this timing model. We then use splk package of TEMPO2 to output timing residual with error bar in unit of second at each TOA. We select 54 pulsars among pulsars regularly monitored at Nanshan with no intention to be make our selection statistically representative. Because of the nature of our analysis method, we mainly select pulsars with small $\dot{P}$ and timing noise like white-noise without recognizable glitch. A list of these pulsars with various parameters (P, $\dot{P}$, dispersion measure and characteristic age τ_c) from the ATNF Pulsar Database (Manchester et al. 2006) is presented Table 1.

3.2 Results and analysis

Using the above methods, Hurst parameters $\{H\}$ and $\{H^{(c)}\}$ with $c = -0.8, -0.4, 0, 0.4, 0.8$ for 54 radio pulsars are calculated. Average values and standard deviations of these two groups of Hurst parameters are listed in Table 2 together with basic parameters of 54 pulsars. Distribution of average $\bar{H}$ is shown in Figure 1. In Figure 2, we plot average value and standard deviation of $\{H\}$ for each pulsar as a black error bar and in comparison average and standard deviation of $\{H^{(c)}\}$ for artificial (anti-)persistent series with $c = \pm 0.8$ and i.i.d. series with $c = 0$ are plotted as connected error bar bands. For clarity we do not show bands of artificial (anti-)persistent series with $c = \pm 0.4$ which roughly fall in the gaps between $c = 0$ and $c = \pm 0.8$ but have some overlap.

From the average and standard deviation of Hurst parameters of the three bands shown in Figure 2, we see that data length and non-uniformity has only limited effect on the Hurst parameter estimation. The values of Hurst parameters of the three groups of artificial series are not exactly the same with Hurst parameters calculated using variance in §2.3. This can be attributed to the difference between calculation by definition and our algorithm using running maximum as mentioned in §2.3.

From these results, we can see that most Hurst parameters for pulsar timing noises concentrate around 0.5. However there are a small portion with H values far away from 0.5 despite considerable data point number. For PSRs J0147+5922, J0357+5236, J0612+3721, J0630−2834, J0823+0159 and J0837−4135 calculated Hurst parameter average $H > 0.75$ and as is shown in Figure 2 their error bars appear together with or even above the $c = 0.8$ band, indicate that they have strong persistent trend. On the other hand, for PSRs J0055+5117, J1022+1001, and J1842−0359

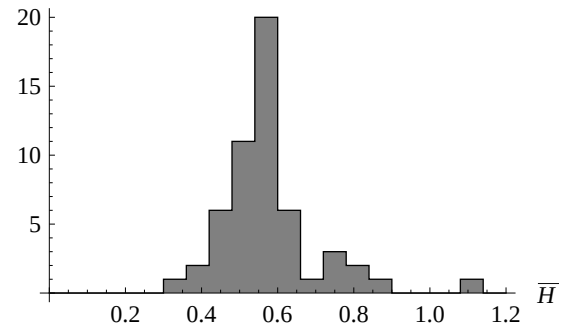

Figure 1. Distribution of Hurst parameters for 54 pulsars. All H values are in the interval $0 \sim 1.2$.

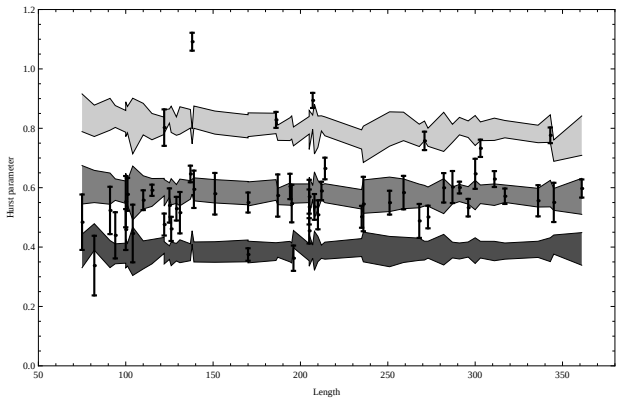

Figure 2. Hurst parameter of 54 pulsars. The black error bar shows average and standard deviation of 1000 Hurst parameter value for each pulsar. In comparison artificial (anti-)persistent series with constant covariance $c = -0.8, 0, 0.8$ are plotted as bands of connected error bars represented by increasing gray level.

calculated Hurst parameter $H < 0.4$ and as is shown in Figure 2 their error bars appear together with or even below the $c = -0.8$ band, indicating strong anti-persistent trend.

To illustrate the typical persistent series and anti-persistent series seen in real pulsar timing noise, we pick three pulsars: PSR J0055+5117 with $H = 0.3749 \pm 0.021$ and $H^{(0)} = 0.5790 \pm 0.081$ representing anti-persistent series, PSR J2108+4441 with $H = 0.5712 \pm 0.026$ and $H^{(0)} = 0.5797 \pm 0.057$ representing independent series and PSR J0357+5236 with $H = 0.8939 \pm 0.025$ and $H^{(0)} = 0.5840 \pm 0.064$ representing persistent series. Their timing noises in unit of millisecond are plotted in Figure 3.

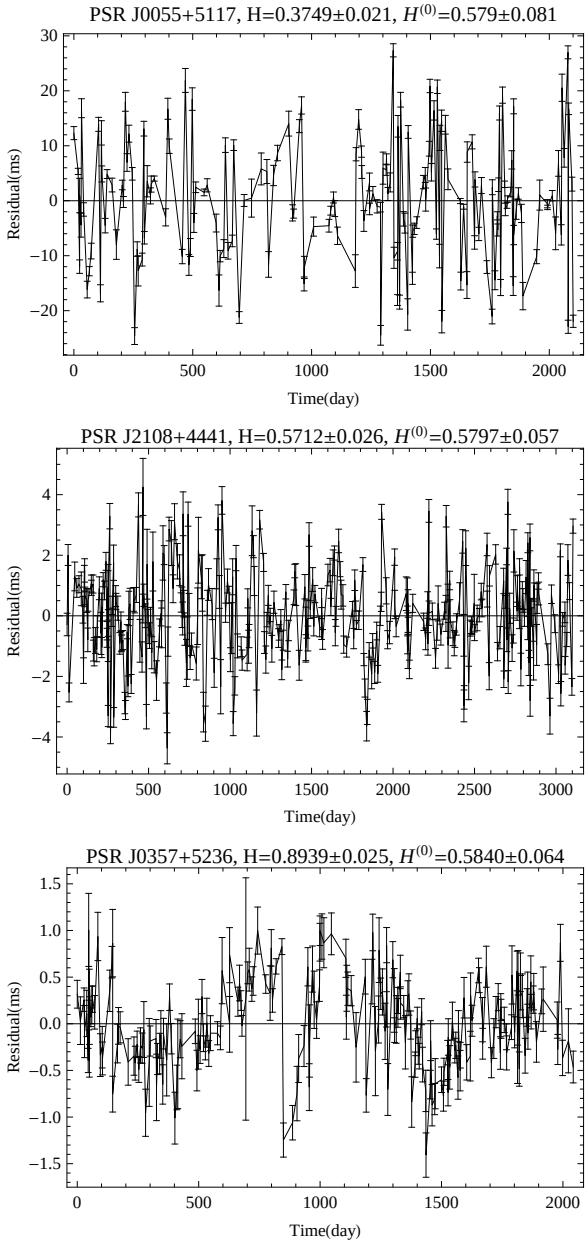

Figure 3. Representative timing noises. PSR J0055+5117 representing anti-persistent series (*top panel*), PSR J2108+4441 representing independent series (*middle panel*), and PSR J0357+5236 representing persistent series (*bottom panel*)

4 DISCUSSION AND CONCLUSION

We calculated Hurst parameter of 54 radio pulsars with white-noise-like timing residual obtained from Nanshan telescope and compared the results with artificial (anti-)persistent series. The majority of pulsars from our selection have Hurst parameters around 0.5 and not far from Hurst parameter calculated for independent series. However, we found 9 pulsars (PSRs J0147+5922, J0357+5236, J0612+3721, J0630−2834, J0823+0159 and J0837−4135 showing persistent trend and PSRs J0055+5117, J1022+1001, and J1842−0359 showing anti-persistent trend) with interesting H values despite having white-noise-like timing residual. Comparison with artificial series confirm that these trends cannot be attributed entirely to effects caused by ROS algorithm or large uncertainty in timing residual. This shows that our algorithm may be capable of detecting hidden correlation in apparently noise-like timing residual. We therefore suggest that these 9 pulsars be monitored continuously to confirm or disprove long-range dependence and search for possible physical process behind such correlation.

As for the selection, we picked 54 pulsars with relatively small period derivative $\dot{P}$, and white-noise-like timing resid-

ual rather than the typical red-noise pattern of the three kind of noise model (PN, FN and SN) first proposed by Boynton et al. (1972) and of course we made no attempt at doing correlation between Hurst parameter and other pulsar properties nor obtaining statistics of Hurst parameter values for large population. Our method is aimed at finding possibility that timing noise that resembles white-noise is not really generated by a random process. As is well known there are pulsars with smooth timing noise that differ largely from white noise (such as J0332+5434, J0406+6138, J0826+2637, etc.) and they would yields quite large Hurst parameter if calculated using our algorithm and some even exceed 1. In that case we do not need the deviation from 0.5 to conclude the obvious dependent nature of timing noise and other method should be used to analyze possible chaotic nature of these timing noise series.

There are various physical processes that might be responsible for the long-range dependence of pulsar timing noise. These can be classified into three groups: from interior of neutron star, i.e. due to fluctuation of internal (e.g. micro-quake due to partial release of elastic energy Pines & Shaham (1972) and random pinning and unpinning of vortex lines Packard (1972), Anderson & Itoh (1975)) and external (e.g. accretion flow Lamb et al. (1978)) torques; from emission process (e.g. magnetosphere activities Cheng (1987)) and from propagation of radio emission. For the last class of origin, it has long been proposed that timing noise can be used to set upper limits on gravitational wave (Bertotti et al. (1983)) and that given enough time pulsar timing array might be the first equipment to directly detect gravitational wave (Manchester (2006)). All of these (including gravitational wave detection which aims at detecting random background) predict randomness in evolution of certain quantity while Hurst parameter is capable of uncovering chaotic behavior that is hidden in timing noise. The physical origin that leads to dependence series is much more limited than random fluctuations. Therefore, long-term dependence detected by Hurst parameter might reveal more detailed information about the physical origin of timing noise. For instance it has been proposed that under certain conditions Euler equations for rotating object with magnetic dipole moment misaligned with rotation axis would show chaotic spin-down behavior (see Harding et al. (1990)). By definition any dynamical process can exhibit chaotic behavior and thus dependence in long-term timing noise data if the system is governed by differential equations whose solution is highly sensitive to initial conditions. We expect that the application of Hurst parameter to timing noise of longer time span reveal more evidence for new physics.

ACKNOWLEDGMENTS

We would like to acknowledge useful discussions at our pulsar group of PKU. This work is supported by NSFC (10778611), the National Basic Research Program of China (grant 2009CB824800) and by LCWR (LHXZ200602).

REFERENCES

Anderson P. W., Itoh N., 1975, Nature, 256, 25
Arzoumanian Z. , Nice D. J., Taylor J. H., Thorsett S. E., 1994, ApJ, 422, 671
Bertotti B., Carr B. J., Rees M. J., 1983, MNRAS, 203, 945
Boynton P. E., Groth E. J., Hutchinson D. P., Nanos G. P., Partridge R. B., Wilkinson D. T., 1972, ApJ, 175, 217
Cheng K. S., 1987, ApJ, 321, 799
Cordes J. M., Greenstein G., 1981, ApJ, 245, 1060
D'Alessandro F., 1990, Ap&SS, 246, 73
Dieker T., 2004, master's thesis, Vrije Universiteit Amsterdam
Feder J., 1988, Fractals, Plenum Press, New York
Harding A. K., Shinbrot T., Cordes J. M., 1990, ApJ, 353, 588
Hobbs G. M., Edwards R. T., Manchester R. N., 2006, MNRAS, 369, 655
Hotan A. W., van Straten W., Manchester R. N., 2004, PASA, 21, 302
Hurst H. E., 1951, Trans Amer Soc Civil Engineers, 116, 770-99
Karatzas I., Shreve S. E., 1991, Brownian Motion and Stochastic Calculus, Springer, p. 94
Lamb F. K., Pines D., Shaham J., 1978, ApJ, 224, 969
Lyne A. G., Smith F. G., 2006, Pulsar Astronomy, Cambridge University Press, p. 74
Manchester R. N. , 2006, ChJAA, 6, 139
Manchester R. N., Hobbs G. B., Teoh A., Hobbs M., 2005, AJ, 129, 1993
Matsumoto M., Nishimura T., 1998, ACM Trans. on Modeling and Computer Simulation, 8, 3
Packard R. E., 1972, Phys. Rev. Lett., 28, 1080
Pines D., Shaham J., 1972, Nature, 235, 43
Steeb W. H., Hardy Y., Stoop R., 2005, The Nonlinear Workbook, World Scientific, p. 123

JName	P(s)	$\dot{P}(10^{-16})$	DM(cm^{-3}·pc)	$\tau_c(10^7 yr)$
J0034−0721	0.94295099	4.0821	11.38	3.66
J0055+5117	2.11517114	95.3764	44.13	0.351
J0134−2937	0.13696158	0.7837	21.81	2.77
J0141+6009	1.22294852	3.9107	34.80	4.95
J0147+5922	0.19632127	2.5677	40.11	1.21
J0151−0635	1.46466454	4.4259	25.66	5.24
J0152−1637	0.83274161	12.992	11.92	1.02
J0215+6218	0.54887981	6.6212	84.00	1.31
J0304+1932	1.38758444	12.9524	15.74	1.7
J0357+5236	0.19703009	4.7659	103.71	0.655
J0502+4654	0.63856548	55.8234	42.19	0.181
J0525+1115	0.35443759	0.7361	79.35	7.63
J0601−0527	0.39596916	13.0210	80.54	0.482
J0612+3721	0.29798232	0.5947	27.14	7.94
J0630−2834	1.24441859	71.229	34.47	0.277
J0758−1528	0.68226517	16.1889	63.33	0.668
J0814+7429	1.29224144	1.6811	6.12	12.2
J0820−1350	1.23812954	21.0518	40.94	0.932
J0823+0159	0.86487280	1.0455	23.73	13.1
J0837+0610	1.27376829	67.9922	12.89	0.297
J0837−4135	0.75162361	35.3930	147.29	0.336
J0846−3533	1.11609716	16.0135	94.16	1.1
J0908−1739	0.40162562	6.6950	15.89	0.95
J0943+1631	1.08741772	0.9109	20.32	18.9
J1022+1001	0.01645292	0.0004	10.25	601
J1041−1942	1.38636807	9.4485	33.78	2.32
J1115+5030	1.65643975	24.9279	9.20	1.05
J1239+2453	1.38244910	9.6005	9.24	2.28
J1257−1027	0.61730766	3.6270	29.63	2.7
J1543+0929	0.74844841	4.3248	35.24	2.74
J1703−3241	1.21178509	6.5983	110.31	2.91
J1733−2228	0.87168283	0.4270	41.14	32.3
J1741−0840	2.04308245	22.7471	74.90	1.42
J1750−3157	0.91036298	1.9652	206.34	7.34
J1756−2435	0.67047996	2.8474	367.10	3.73
J1820−1818	0.30990459	0.9361	436	5.25
J1822−2256	1.87426851	13.5439	121.20	2.19
J1823+0550	0.75290654	2.2673	66.78	5.26
J1834−0426	0.29010819	0.7195	79.31	6.39
J1837−0653	1.90580870	7.7204	316	3.91
J1840+5640	1.65286185	14.9482	26.70	1.75
J1842−0359	1.83994431	5.0876	195.98	5.73
J1852−2610	0.33633713	0.8771	56.81	6.08
J1900−2600	0.61220920	2.0453	37.99	4.74
J1901−0906	1.78192776	16.3829	72.68	1.72
J1921+2153	1.33730216	13.4821	12.46	1.57
J1946+1805	0.44061847	0.2409	16.22	29
J1954+2923	0.42667678	0.0171	7.93	395
J2018+2839	0.55795348	1.4811	14.17	5.97
J2046−0421	1.54693811	14.7148	35.80	1.67
J2046+1540	1.13828568	1.8232	39.84	9.89
J2108+4441	0.41487053	0.8621	139.83	7.62
J2113+4644	1.01468479	7.1461	141.26	2.25
J2308+5547	0.47506767	1.9949	46.54	3.77

Table 1. Parameters of 54 pulsars used in Hurst parameter calculation from ATNF Pulsar Catalog (Manchester et al. 2006)

JName	H	$H^{(-0.8)}$	$H^{(-0.4)}$	$H^{(0)}$	$H^{(0.4)}$	$H^{(0.8)}$
J0034−0721	0.5500 ± 0.034	0.3872 ± 0.073	0.5123 ± 0.077	0.5817 ± 0.079	0.6627 ± 0.081	0.8067 ± 0.078
J0055+5117	0.3749 ± 0.021	0.3833 ± 0.073	0.5143 ± 0.078	0.5790 ± 0.081	0.6589 ± 0.083	0.8120 ± 0.080
J0134−2937	0.4612 ± 0.041	0.3772 ± 0.079	0.5094 ± 0.083	0.5861 ± 0.088	0.6731 ± 0.093	0.8302 ± 0.088
J0141+6009	0.5327 ± 0.030	0.3917 ± 0.051	0.5099 ± 0.055	0.5741 ± 0.059	0.6514 ± 0.057	0.7969 ± 0.056
J0147+5922	0.8283 ± 0.027	0.3847 ± 0.060	0.5103 ± 0.068	0.5923 ± 0.069	0.6703 ± 0.073	0.8164 ± 0.069
J0151−0635	0.4837 ± 0.093	0.3870 ± 0.110	0.5185 ± 0.120	0.6097 ± 0.130	0.6938 ± 0.130	0.8522 ± 0.130
J0152−1637	0.5945 ± 0.063	0.3835 ± 0.068	0.5119 ± 0.074	0.5944 ± 0.077	0.6807 ± 0.079	0.8375 ± 0.075
J0215+6218	0.6041 ± 0.043	0.3847 ± 0.069	0.5085 ± 0.073	0.5783 ± 0.075	0.6554 ± 0.080	0.7971 ± 0.077
J0304+1932	0.5465 ± 0.063	0.3802 ± 0.067	0.5044 ± 0.073	0.5750 ± 0.075	0.6472 ± 0.076	0.8025 ± 0.078
J0357+5236	0.8939 ± 0.025	0.3847 ± 0.057	0.5121 ± 0.063	0.5840 ± 0.064	0.6678 ± 0.065	0.8204 ± 0.064
J0502+4654	0.6647 ± 0.036	0.3879 ± 0.060	0.5090 ± 0.064	0.5815 ± 0.065	0.6630 ± 0.069	0.8067 ± 0.065
J0525+1115	0.5351 ± 0.059	0.3827 ± 0.063	0.5058 ± 0.067	0.5812 ± 0.070	0.6620 ± 0.073	0.8101 ± 0.066
J0601−0527	0.5020 ± 0.037	0.3983 ± 0.080	0.5063 ± 0.081	0.5609 ± 0.089	0.6291 ± 0.093	0.7625 ± 0.093
J0612+3721	0.7576 ± 0.031	0.3880 ± 0.056	0.5051 ± 0.061	0.5730 ± 0.063	0.6457 ± 0.066	0.7913 ± 0.063
J0630−2834	0.7764 ± 0.026	0.3912 ± 0.045	0.5098 ± 0.049	0.5800 ± 0.050	0.6519 ± 0.052	0.7991 ± 0.050
J0758−1528	0.7326 ± 0.029	0.3913 ± 0.053	0.5076 ± 0.059	0.5777 ± 0.057	0.6516 ± 0.061	0.7899 ± 0.061
J0814+7429	0.5972 ± 0.031	0.3938 ± 0.054	0.5076 ± 0.056	0.5708 ± 0.059	0.6352 ± 0.059	0.7753 ± 0.058
J0820−1350	0.5560 ± 0.052	0.3924 ± 0.054	0.5042 ± 0.058	0.5663 ± 0.058	0.6365 ± 0.062	0.7810 ± 0.059
J0823+0159	1.0916 ± 0.030	0.4322 ± 0.130	0.5432 ± 0.140	0.6033 ± 0.150	0.6642 ± 0.160	0.7727 ± 0.170
J0837+0610	0.6022 ± 0.054	0.3900 ± 0.058	0.5007 ± 0.060	0.5737 ± 0.065	0.6407 ± 0.065	0.7830 ± 0.064
J0837−4135	0.8023 ± 0.061	0.4057 ± 0.100	0.5270 ± 0.110	0.6020 ± 0.110	0.6701 ± 0.120	0.8085 ± 0.120
J0846−3533	0.6004 ± 0.020	0.3868 ± 0.049	0.5107 ± 0.053	0.5821 ± 0.055	0.6602 ± 0.054	0.8074 ± 0.051
J0908−1739	0.5353 ± 0.043	0.3875 ± 0.064	0.5080 ± 0.074	0.5760 ± 0.074	0.6552 ± 0.073	0.7975 ± 0.072
J0943+1631	0.5401 ± 0.058	0.3814 ± 0.073	0.5148 ± 0.077	0.5922 ± 0.084	0.6830 ± 0.085	0.8413 ± 0.081
J1022+1001	0.3625 ± 0.043	0.4268 ± 0.100	0.5277 ± 0.110	0.5802 ± 0.120	0.6448 ± 0.120	0.7727 ± 0.130
J1041−1942	0.5449 ± 0.092	0.4003 ± 0.085	0.5129 ± 0.097	0.5699 ± 0.099	0.6261 ± 0.110	0.7460 ± 0.110
J1115+5030	0.5736 ± 0.071	0.3905 ± 0.077	0.5102 ± 0.088	0.5703 ± 0.090	0.6463 ± 0.090	0.7851 ± 0.092
J1239+2453	0.5504 ± 0.066	0.4084 ± 0.077	0.5095 ± 0.083	0.5605 ± 0.083	0.6112 ± 0.084	0.7249 ± 0.089
J1257−1027	0.5695 ± 0.057	0.3839 ± 0.068	0.5077 ± 0.074	0.5796 ± 0.075	0.6499 ± 0.078	0.7999 ± 0.073
J1543+0929	0.5890 ± 0.031	0.3843 ± 0.059	0.5064 ± 0.064	0.5843 ± 0.063	0.6650 ± 0.067	0.8165 ± 0.062
J1703−3241	0.5996 ± 0.049	0.3912 ± 0.057	0.5099 ± 0.063	0.5715 ± 0.062	0.6485 ± 0.061	0.7880 ± 0.063
J1733−2228	0.5086 ± 0.049	0.3933 ± 0.069	0.5086 ± 0.074	0.5751 ± 0.079	0.6484 ± 0.079	0.7886 ± 0.078
J1741−0840	0.5158 ± 0.070	0.3860 ± 0.082	0.5153 ± 0.088	0.5840 ± 0.094	0.6725 ± 0.098	0.8264 ± 0.089
J1750−3157	0.5775 ± 0.055	0.3743 ± 0.094	0.5032 ± 0.100	0.5832 ± 0.110	0.6694 ± 0.110	0.8291 ± 0.110
J1756−2435	0.5530 ± 0.086	0.3795 ± 0.100	0.5120 ± 0.110	0.5847 ± 0.120	0.6703 ± 0.120	0.8234 ± 0.120
J1820−1818	0.5292 ± 0.040	0.3828 ± 0.089	0.5099 ± 0.100	0.5790 ± 0.110	0.6476 ± 0.110	0.8074 ± 0.110
J1822−2256	0.6462 ± 0.028	0.3826 ± 0.075	0.5088 ± 0.084	0.5925 ± 0.090	0.6767 ± 0.084	0.8320 ± 0.079
J1823+0550	0.5796 ± 0.070	0.3834 ± 0.075	0.5075 ± 0.078	0.5879 ± 0.080	0.6672 ± 0.087	0.8193 ± 0.075
J1834−0426	0.5913 ± 0.019	0.3845 ± 0.097	0.5116 ± 0.110	0.5839 ± 0.110	0.6610 ± 0.120	0.8057 ± 0.120
J1837−0653	0.5578 ± 0.033	0.3736 ± 0.085	0.5095 ± 0.094	0.5842 ± 0.100	0.6730 ± 0.099	0.8310 ± 0.096
J1840+5640	0.5495 ± 0.040	0.3848 ± 0.057	0.5054 ± 0.061	0.5776 ± 0.065	0.6550 ± 0.063	0.7976 ± 0.061
J1842−0359	0.3376 ± 0.100	0.4340 ± 0.160	0.5390 ± 0.180	0.6040 ± 0.180	0.6759 ± 0.190	0.8252 ± 0.190
J1852−2610	0.4759 ± 0.037	0.3807 ± 0.087	0.5111 ± 0.096	0.5829 ± 0.099	0.6737 ± 0.100	0.8229 ± 0.100
J1900−2600	0.4881 ± 0.057	0.3927 ± 0.067	0.5042 ± 0.068	0.5722 ± 0.072	0.6328 ± 0.074	0.7762 ± 0.074
J1901−0906	0.4590 ± 0.069	0.3787 ± 0.091	0.5126 ± 0.097	0.5911 ± 0.110	0.6725 ± 0.100	0.8306 ± 0.110
J1921+2153	0.5835 ± 0.056	0.3906 ± 0.055	0.5063 ± 0.059	0.5793 ± 0.059	0.6565 ± 0.063	0.8064 ± 0.058
J1946+1805	0.5013 ± 0.038	0.3912 ± 0.065	0.5038 ± 0.071	0.5700 ± 0.073	0.6339 ± 0.074	0.7699 ± 0.075
J1954+2923	0.4457 ± 0.097	0.3859 ± 0.110	0.5106 ± 0.120	0.5822 ± 0.130	0.6664 ± 0.130	0.8076 ± 0.130
J2018+2839	0.6467 ± 0.051	0.3881 ± 0.053	0.5038 ± 0.056	0.5752 ± 0.058	0.6462 ± 0.062	0.7925 ± 0.059
J2046−0421	0.4396 ± 0.078	0.3773 ± 0.092	0.5101 ± 0.098	0.5934 ± 0.110	0.6838 ± 0.110	0.8398 ± 0.100
J2046+1540	0.5234 ± 0.080	0.3764 ± 0.094	0.5105 ± 0.100	0.5968 ± 0.110	0.6855 ± 0.110	0.8472 ± 0.110
J2108+4441	0.5712 ± 0.026	0.3865 ± 0.049	0.5087 ± 0.051	0.5797 ± 0.057	0.6532 ± 0.053	0.7972 ± 0.052
J2113+4644	0.6291 ± 0.027	0.3867 ± 0.051	0.5061 ± 0.053	0.5764 ± 0.056	0.6476 ± 0.058	0.7967 ± 0.054
J2308+5547	0.4547 ± 0.043	0.3892 ± 0.071	0.5030 ± 0.076	0.5710 ± 0.078	0.6508 ± 0.080	0.7945 ± 0.080

Table 2. Hurst parameters for timing noise series of 54 pulsars together with 5 artificial (anti-)persistent series for comparison. See §2.3 for explanation of symbols.